Determining the final spin of a binary black hole system including in-plane spins: Method and checks of accuracy

Nathan K. Johnson-McDaniel,[1] Anuradha Gupta,[2] P. Ajith,[1] David Keitel,[3] Ofek Birnholtz,[4] Frank Ohme,[5] and Sascha Husa[3]

[1]*International Centre for Theoretical Sciences, Tata Institute of Fundamental Research, Bengaluru 560089, India*
[2]*Inter-University Centre for Astronomy and Astrophysics, Pune 411007, India*
[3]*Universitat de les Illes Balears and Institut d'Estudis Espacials de Catalunya, 07122 Palma, Spain*
[4]*Albert-Einstein-Institut, Max-Planck-Institut für Gravitationsphysik, 30167 Hannover, Germany*
[5]*Cardiff University, Cardiff CF24 3AA, United Kingdom*

(Dated: May 25, 2016)

We describe a simple extension to aligned-spin fits for the final spin of a binary black hole system that includes the contribution from the in-plane spins. We show that this addition gives good agreement with the final spin from a suite of 752 numerical relativity simulations when applied to the aligned-spin fit from Healy, Lousto, and Zlochower (HLZ) [1]. This agreement is increased if one evolves the spins using post-Newtonian expressions. We also show that the unmodified HLZ final mass fit gives good agreement with the numerical relativity data.

I. THE FINAL SPIN EXPRESSION

We can augment aligned-spin fits for the final spin to include the contribution from the in-plane spins in a simple way (first introduced in [2]). The basic idea is the same as that used in the precessing IMRPhenom waveform model (introduced in an earlier form in [3]) to extend the IMRPhenomD aligned-spin fit [4] to the precessing case (see [5]):[1]

$$\chi_f^{\text{full}} = \sqrt{\left(\chi_f^{\text{aligned}}\right)^2 + \left(S^{\text{in-plane}}/M^2\right)^2}. \tag{1}$$

Here χ_f^{aligned} is the final (dimensionless) spin obtained from the fit using the components of the spins along the orbital angular momentum, $S^{\text{in-plane}}$ is the magnitude of the sum of the in-plane components of the dimensionful spins, and M is the binary's initial (total) mass. Using the initial mass gives better agreement with the numerical relativity (NR) data than does using the final mass. Additionally, if one uses the initial mass, one obtains a χ_f^{full} that is always less than the Kerr bound of 1 when using either the Healy, Lousto, and Zlochower (HLZ) [1] or IMRPhenomD aligned-spin fits, even for extremal initial spins. This is not the case if one uses the final mass.

One can obtain even better agreement with NR results if one uses post-Newtonian expressions to evolve the initial spins up to orbital velocity of the Schwarzschild innermost stable circular orbit (ISCO), i.e., $v = 6^{-1/2} \simeq 0.41$, before applying Eq. (1). Here we use the expressions from [7]. When evolving parameter estimation samples, we initialize the evolution using f_{ref} (the $2, 2$ mode gravitational wave frequency at which the spins are defined in the waveform; 20 Hz for O1 analyses) to set the binary's initial orbital velocity by $v_0 = (\pi M_z f_{\text{ref}})^{1/3}$. Here we use the binary's redshifted mass M_z, since f_{ref} is defined in the detector frame.

When comparing with NR simulations, we either use $M\omega_0$ (obtained from the initial frequency of the waveform) instead of $\pi M_z f_{\text{ref}}$ or, if this is not available, the magnitude of the initial orbital angular momentum, L_0, using the first post-Newtonian (1PN) relation $v_0 = M\eta/L_0 + (3/2 + \eta/6)(M\eta/L_0)^3$, where M is the total mass and η is the symmetric mass ratio. Note that this evolution only affects the final spin in double spin cases: The post-Newtonian evolution equations we use preserve the component of the spin along the orbital angular momentum in single spin cases. We also use the direction of the initial orbital angular momentum from the numerical simulation (obtained from the initial ADM angular momentum $\boldsymbol{J}_{\text{ADM}}$ and the coordinate components of the binary's dimensionful spins $\boldsymbol{S}_{1,2}$ by $\boldsymbol{L}_0 = \boldsymbol{J}_{\text{ADM}} - \boldsymbol{S}_1 - \boldsymbol{S}_2$ if not given explicitly) to initialize the spin evolution when available; when it is not available, we take it to be in the z-direction.

II. COMPARISON WITH NUMERICAL RELATIVITY

We compare with 752 numerical relativity simulations from four different collaborations, including 473 precessing simulations with mass ratios up to 8 and dimensionless spins up to 0.8 in most cases; a few have spins of up to 0.99 on one hole. We use the 144 quasicircular simulations (eccentricity $< 10^{-3}$) from the Simulating eXtreme Spacetimes catalogue (using the SpEC code) [8, 9] and the 341 simulations from the Georgia Institute of Technology catalogue (using the Maya code) [10, 11] that

[1] Note, however, that the IMRPhenomPv2 final spin expression computes the in-plane spin from χ_p, while we compute it from the spin magnitudes, tilt angles, and ϕ_{12}; these are defined in [6].

give final mass and spin data (leaving off GT0392, which is the shortest waveform in the catalogue, and whose final spin has uncertain accuracy). Additionally, we use 244 simulations from the Rochester Institute of Technology group (using the LAZEV code [12])—the 140 simulations from [13] plus 104 further simulations, many of which are currently unpublished [14]—and 23 unpublished precessing simulations by the Cardiff University and Universitat de les Illes Balaers groups (using the BAM code [15, 16]) with parameters close to those inferred for GW150914.

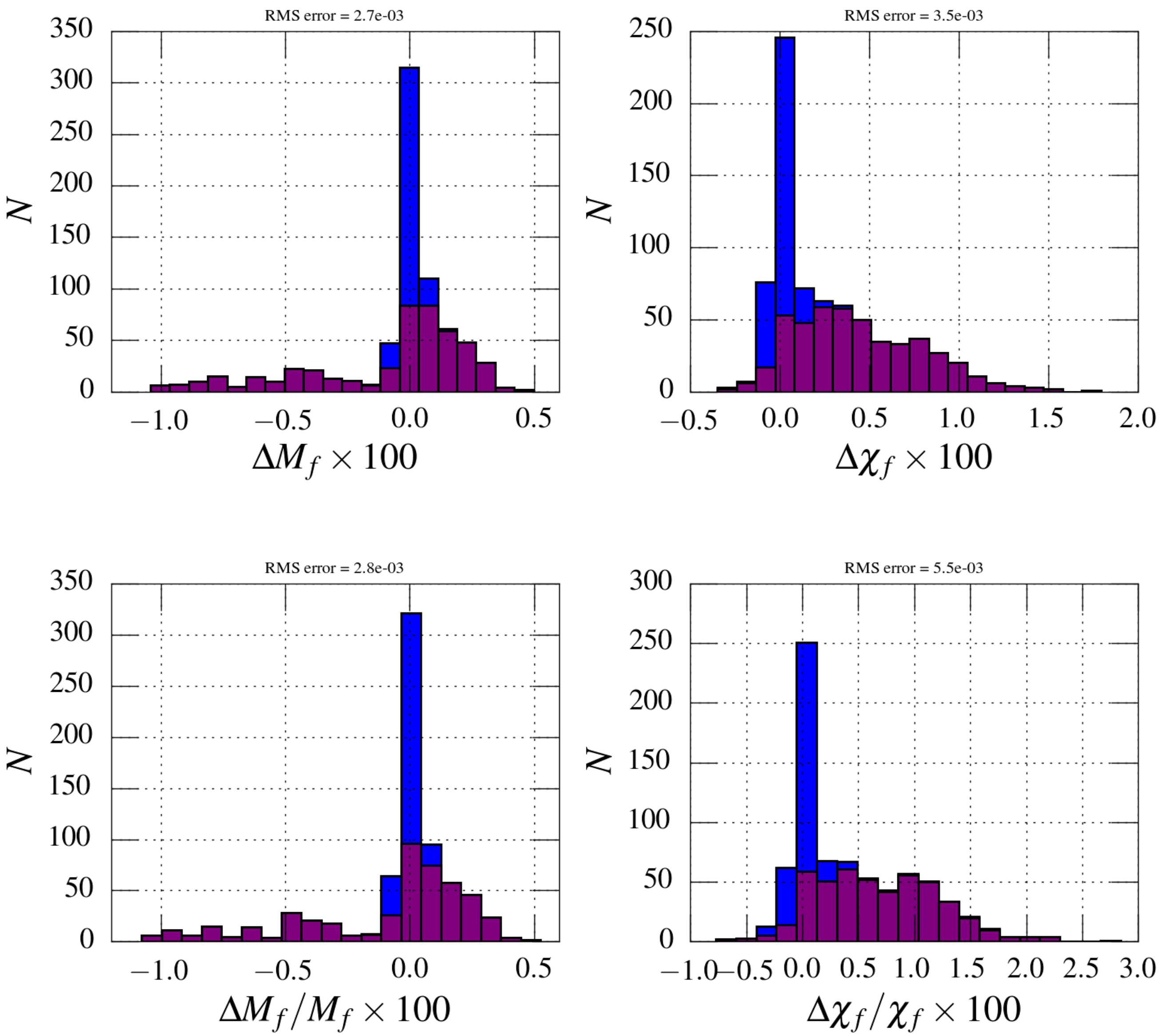

FIG. 1. Histograms of absolute *(top)* and fractional *(bottom)* errors in the final mass and spin comparing to all the simulations we consider using the augmented HLZ fit with spin evolution. We show just precessing simulations in purple and all simulations in blue.

In Fig. 1 we show a histogram of the errors (absolute and fractional) in the final mass and spin when comparing with the HLZ fit, with the final spin augmented with the in-plane spins using spin evolution, as described above, and the final mass fit evaluated using the components of the spins along the orbital angular momentum. When computing the histogram of fractional errors on the final spin, we omit a few cases with final spin magnitudes < 0.05, for which there is a large fractional error, even though the magnitude of the absolute error is $\lesssim 0.002$. We compute the errors as fit $-$ data and denote the final mass and (dimensionless) spin by M_f and χ_f, respectively.

The 90% confidence intervals for the error on χ_f are $[-1.1, 8.4] \times 10^{-3}$ (absolute) and $[-2.3, 12] \times 10^{-2}$ (fractional). For M_f they are $[-8.1, 3.4] \times 10^{-3}$ (absolute) and $[-5.2, 3.7] \times 10^{-3}$ (fractional). Even if we just restrict to all the precessing systems, the 90% confidence intervals for the errors on χ_f are $[-1.1, 9.5] \times 10^{-3}$ (absolute) and $[-0.5, 14] \times 10^{-3}$ (fractional), while the errors on M_f are almost unchanged: The only difference is the lower bound for the fractional errors, which becomes -8.4×10^{-3}.

ACKNOWLEDGMENTS

We acknowledge the Simulating eXtreme Spacetimes project and Georgia Institute of Technology for their public NR waveform catalogues, and the following people for providing us with results from yet-to-be-published simulations: Edward Fauchon-Jones, Mark Hannam, Chinmay Kalaghatgi, Sebastian Khan, Lionel London, Francesco Pannarale, and Alex Vano-Vinuales (Cardiff University); Manuela Campanelli, James Healy, Carlos Lousto, and Yosef Zlochower (Rochester Institute of Technology).

[1] J. Healy, C. O. Lousto, and Y. Zlochower, Phys. Rev. D, **90**, 104004 (2014), arXiv:1406.7295 [gr-qc].

[2] L. Rezzolla, E. Barausse, E. N. Dorband, D. Pollney, C. Reisswig, J. Seiler, and S. Husa, Phys. Rev. D, **78**, 044002 (2008), arXiv:0712.3541 [gr-qc].

[3] M. Hannam, P. Schmidt, A. Bohé, L. Haegel, S. Husa, F. Ohme, G. Pratten, and M. Pürrer, Phys. Rev. Lett., **113**, 151101 (2014), arXiv:1308.3271 [gr-qc].

[4] S. Husa, S. Khan, M. Hannam, M. Pürrer, F. Ohme, X. Jiménez Forteza, and A. Bohé, Phys. Rev. D, **93**, 044006 (2016), arXiv:1508.07250 [gr-qc].

[5] `http://software.ligo.org/docs/lalsuite/lalsimulation/_l_a_l_sim_i_m_r_phenom_p_8c.html#ab2eda2f4843bc0ecd5a5d9660877d50e`.

[6] B. Farr, E. Ochsner, W. M. Farr, and R. O'Shaughnessy, Phys. Rev. D, **90**, 024018 (2014), arXiv:1404.7070 [gr-qc].

[7] P. Ajith, Phys. Rev. D, **84**, 084037 (2011), arXiv:1107.1267 [gr-qc].

[8] A. H. Mroué *et al.*, Phys. Rev. Lett., **111**, 241104 (2013), arXiv:1304.6077 [gr-qc].

[9] `http://www.black-holes.org/waveforms/`.

[10] K. Jani, J. Healy, J. A. Clark, L. London, P. Laguna, and D. Shoemaker, (2016), arXiv:1605.03204 [gr-qc].

[11] `http://www.einstein.gatech.edu/catalog/`.

[12] Y. Zlochower, J. G. Baker, M. Campanelli, and C. O. Lousto, Phys. Rev. D, **72**, 024021 (2005), arXiv:gr-qc/0505055 [gr-qc].

[13] Y. Zlochower and C. O. Lousto, Phys. Rev. D, **92**, 024022 (2015), arXiv:1503.07536 [gr-qc].

[14] J. Healy, C. O. Lousto, *et al.*, (in preparation).

[15] B. Brügmann, J. A. Gonzalez, M. Hannam, S. Husa, U. Sperhake, and W. Tichy, Phys. Rev. D, **77**, 024027 (2008), arXiv:gr-qc/0610128 [gr-qc].

[16] S. Husa, J. A. Gonzalez, M. Hannam, B. Brügmann, and U. Sperhake, Classical Quantum Gravity, **25**, 105006 (2008), arXiv:0706.0740 [gr-qc].